Cannabidiol as an OX1R Antagonist

The potential, multifaceted therapeutic profile of cannabidiol (CBD), a major constituent derived from the Cannabis sativa plant, covers a wide range of neurological and psychiatric disorders, ranging from anxiety to pediatric epilepsy and drug addiction. However, the molecular targets responsible for these effects have been only partially identified. In this view, the involvement of the orexin system, the key regulator in arousal and the sleep/wake cycle, and in motivation and reward processes, including drug addiction, prompted us to explore, using computational and experimental approaches, the possibility that CBD could act as a ligand of orexin receptors, orexin 1 receptor of type 1 (OX1R) and type 2 (OX2R). Ligand-binding assays showed that CBD is a selective ligand of OX1R in the low micromolar range (Ki 1.58 ± 0.2 μM) while in vitro functional assays, carried out by intracellular calcium imaging and mobilization assays, showed that CBD acts as an antagonist at this receptor. Finally, the putative binding mode of CBD has been inferred by molecular docking and molecular dynamics simulations and its selectivity toward the OX1R subtype rationalized at the molecular level. This study provides the first evidence that CBD acts as an OX1R antagonist, supporting its potential use in addictive disorders and/or body weight regulation.

Keywords: orexin receptors ; cannabidiol ; molecular docking ; molecular dynamics ; calcium mobilization assay

1. Introduction

Cannabidiol (CBD), the main non-euphoric constituent of *Cannabis sativa,* exhibits a complex neuropharmacological profile, ranging from anxiolytic, anticonvulsive, and neuroprotective properties to analgesic and anti-inflammatory effects, all potentially useful for the treatment of several neurological and psychiatric disorders [1][2]. The molecular targets of CBD likely involved in its therapeutic effects have been recently reviewed [3][4] and include, among others, the transient potential receptor channels (TRPs) TRPV1, TRPA1, and TRPM8 [5], the G-protein coupled receptors GPR55 [6], serotonin 1A receptor [7], and opioid receptors [8]. Moreover, even though CBD has a low affinity for the cannabinoid receptors, recent evidence indicated that it may act as a cannabinoid receptor of type 1 (CB1R)-negative allosteric modulator in some circumstances [9][10][11]. More recently, CBD has been also proposed as a therapeutic tool for addictive disorders such as drug and alcohol abuse [12][13][14]. In this view, the recent findings that the orexin system is involved in drug addiction [15], prompted us to investigate the orexin receptors, OX1R and OX2R, as possible targets for CBD. Both receptors are coupled with a Gq protein and their activation induces cell responses mainly via calcium (Ca^{2+})- and diacylglycerol (DAG)-mediated pathways [16][17]. The endogenous ligands of these G-protein coupled receptors are two hypothalamic neuropeptides, orexin-A (OX-A) and orexin-B (OX-B), which regulate different physiological functions in mammals, such as sleep-wake cycles, energy metabolism, and feeding [18]. Both peptides arise from a common precursor, the prepro-orexin, a 130-amino-acid peptide. Orexin projections extend widely throughout the brain, innervating the neocortex, hippocampus, and forebrain structures implicated in the processing of arousal [19], wakefulness [20], feeding [21], emotion, and motivation [22]. Defects in the orexin system induce narcolepsy and catalepsy, whereas inhibitors of orexin receptors represent a promising therapy for the treatment of sleep disorders [23]. Orexin 1 and Orexin 2 receptors are differently distributed in the central nervous system (CNS), thus reflecting different biological profiles—while OX2R is mainly involved in sleep and arousal, OX1R is implicated in compulsive behaviour related to drug addiction and anxiety [24]. OX1R has a higher affinity for OX-A than OX-B, whereas OX2R binds both OX-A and OX-B with the same affinity [23]. In the present study, by performing binding experiments on both orexin receptors, we found that CBD binds OX1R selectively over OX2R. Then, by exploiting the recently-released X-ray structures of both orexin receptors [25][26], the putative binding modes of CBD to OX1R were investigated by molecular docking and molecular dynamics simulations. Computational data, in addition to providing a possible structural basis for the observed binding, also allowed a rationalization of CBD selectivity toward the OX1R subtype. Finally, functional studies based on the measurement of intracellular calcium imaging and mobilization in OX1R-transfected Chinese hamster ovary (CHO) cells allowed the characterization of CBD as an OX1R antagonist.

2. Discussion

The molecular mechanisms responsible for the complex pharmacology of phytocannabinoids in general, including CBD, are still far from being fully understood. Since CBD has received attention for the treatment of drug addiction [12], we considered the orexin receptors as putative molecular targets for this phytocannabinoid. Indeed, biochemical and pharmacological studies [27][28] showed that not only does a cross-talk exist between the endocannabinoid and the hypocretinergic systems, but also that CB_1R and OX1R receptors form heterodimers, suggesting a synergistic or a mutual modulatory role in common physiopathological functions. In this study, we investigated whether CBD acts as a ligand of orexin receptors.

### 2.1. Radioligand Binding Assay

The affinity of CBD for both OX1R and OX2R was tested on CHO cells overexpressing either receptor. As described by the four-parameter logistic fit (**Figure 1**), CBD displaced [^{125}I] OX-A binding at the OX1R in a concentration-dependent manner with a K_i of 1.58 ± 0.2 μM. However, at OX2Rs, CBD was able to only partially (28.0 +/− 8.3%) (n = 3) displace such binding at the highest concentration examined (10 μM). Thus, radioligand binding assay showed that CBD selectively binds to OX1R with a K_i of 1.58 ± 0.2 μM, a value very close to the clinically achieved concentration (healthy volunteers who received CBD oral solution ~21.4 mg/kg/day for six days achieved a plasma Cmax of 330.3 ng/mL, which equates to 1.04 μM) [29].
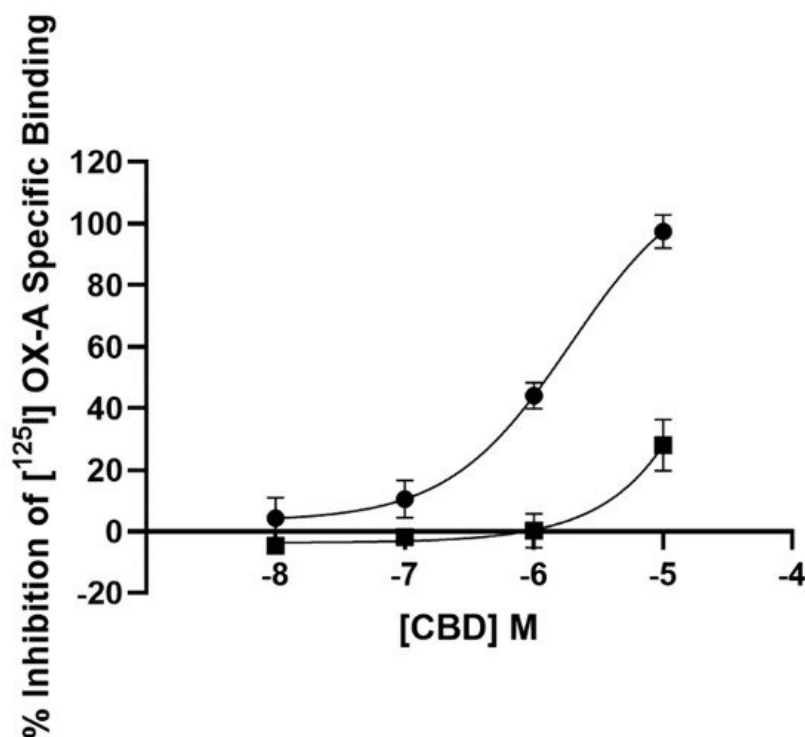

Figure 1. Competition for [^{125}I] orexin-A binding to OX1R-CHO cells (filled circle) and OX2R-CHO cells (filled square) by CBD. Data are the mean of three independent experiments; vertical lines show standard deviation.

2.2. Calcium Mobilization Assay

Ca^{2+} elevations in OX1-CHO cells were measured using the fluorescent Ca^{2+} indicator Fluo-4. Preincubation (5 min) of OX1R-CHO cells with different doses of CBD, followed by incubation with OX-A (100 nM) in 1.5 mM of extracellular Ca^{2+}, caused inhibition of the Ca^{2+} elevation due to OX1R response to OX-A. The corresponding dose-inhibition curve is reported in **Figure 2** and showed an IC_{50} value of 4.2 ± 0.2 μM (n = 5). The OX1R antagonist SB334867 at 10 μM was used as a reference compound to assess the specificity of the antagonist activity of CBD and the inhibition graph is shown in **Figure 3**. We also tested CBD and OXA in not-transfected CHO cells. In both transfected and not transfected CHO cells CBD caused a slight but significant elevation of intracellular calcium. This effect has been previously reported in several cell types and appears to be independent of direct interaction with Gq [30][31].
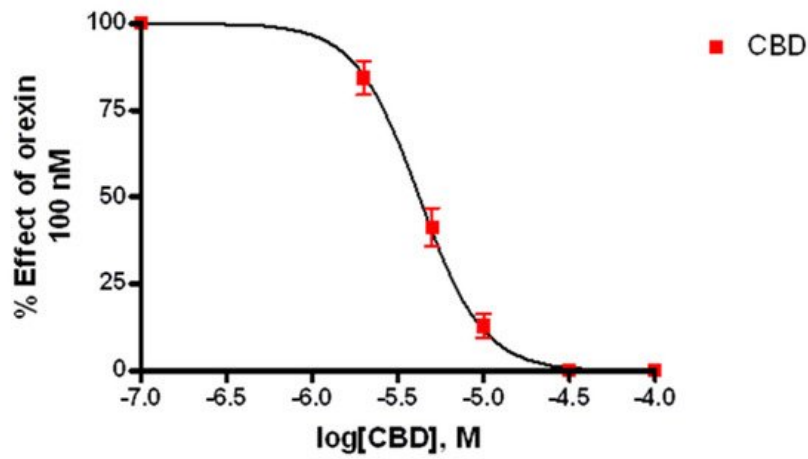
Figure 2. Effect of CBD on Ca^{2+} elevation induced by 100 nM OX-A in CHO cells overexpressing OX1R. Data (mean ± SEM of five independent experiments) are expressed as a percent of the maximal effect observed with OX-A alone (see **Figure 3**); vertical lines show SEM.
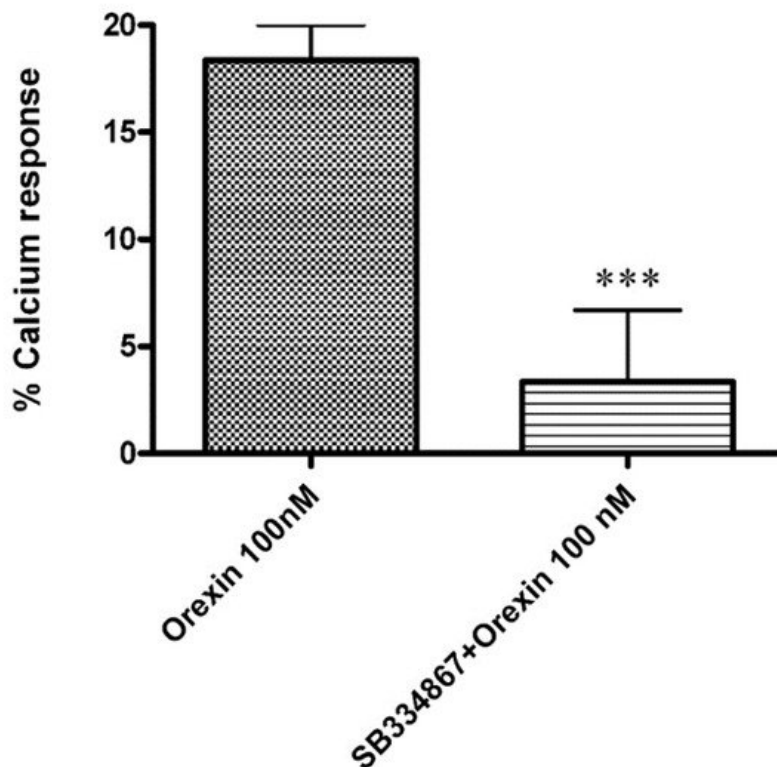

Figure 3. Effect of the OX1R antagonist SB334867 (10 µM) on the Ca^{2+} elevation induced by OX-A (100 nM) in CHO cells overexpressing OX1R. Data are expressed as means ± SEM, ($n = 4$). *** $p < 0.01$.

2.3. Calcium Imaging

2.3.1. OX-A Increases Intracellular $[Ca^{2+}]_i$ in CHO Cells Stably Expressing OX1R or OX2R

OX1R-CHO or OX2R-CHO cells were used for $[Ca^{2+}]_i$ measurements with fFura-2 fluorescence imaging. OX-A was used at a concentration of 200 nM (chosen according to the effective doses used in our previous study [28]). This concentration of OX-A induced a $[Ca^{2+}]_i$ increase with a peak of $[Ca^{2+}]_i$ significantly higher than the basal $[Ca^{2+}]_i$, both in OX1R-CHO (peak $[Ca^{2+}]_i$: 81.5 ± 6.1 nM vs. basal $[Ca^{2+}]_i$: 7.3 ± 1.6 nM; $p < 0.001$) and OX2R-CHO (peak $[Ca^{2+}]_i$: 80.1 ± 5.7 nM vs. basal $[Ca^{2+}]_i$: 9.1 ± 1.8 nM; $p < 0.001$) cells. OX-A-induced $[Ca^{2+}]_i$ increase took place in a fast manner (50–60 s), as shown in a representative graph referred to a randomly recorded single CHO cell stably expressing OX1R (**Figure 4**A) or OX2R (**Figure 5**A). The CHO cells stably expressing OX1R did not show $[Ca^{2+}]_i$ increases in response to 200 nM OXA applied for 180 s after 180 s of treatment with the OX1R antagonist SB334867 (10 µM) in the cell medium (**Figure 4**B). These results indicate that OX-A directly targets OX1R to regulate $[Ca^{2+}]_i$ increase in CHO cells stably expressing OX1R. As shown in **Figure 5**B, and in agreement with its partial antagonistic effect on OX2R, incubation of OX2R-CHO cells with SB334867 10 µM in the calcium-containing buffer solution was able to only partially block the $[Ca^{2+}]_i$ elevation induced by 200 nM OX-A (peak $[Ca^{2+}]_i$: 25.7 ± 3.4 nM vs. basal $[Ca^{2+}]_i$: 7.1 ± 2.6 nM; $p < 0.05$).
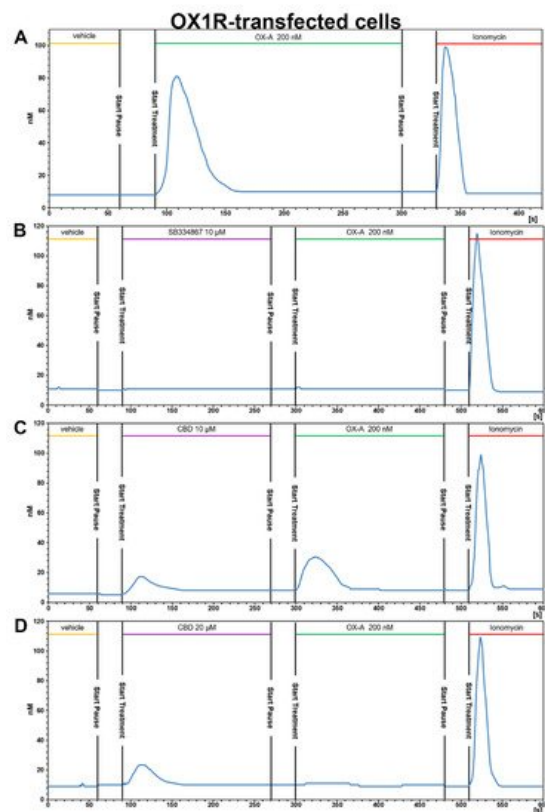
Figure 4. CBD prevents the OX-A-induced $[Ca^{2+}]_i$ response in CHO cells expressing OX1R. Representative traces of single-cell $[Ca^{2+}]_i$ response in Fura-2- loaded CHO cells stably expressing OX1R treated with 200 nM OXA, alone or in combination with 10 µM SB334867 or with 10 µM or 20 µM CBD, and finally with ionomycin (2 µM). Images, collected continuously for 420 s (**A**,**B**) or 600 s (**C**,**D**), were analyzed by the Leica MetaMorph software for calcium imaging to quantify the intracellular $[Ca^{2+}]_i$ increase expressed as 340/387 nm excitation ratio between calcium-bound Fura-2 (green cells) and calcium-free Fura-2 (red cells). (A) 200 nM OX-A increases $[Ca^{2+}]_i$ in cells. (**B**) The OX1R antagonist SB334867 prevents the OX-A-induced $[Ca^{2+}]_i$ enhancement in the cells. OX-A-responsive cells became partially (**C**) or completely (**D**) unresponsive to 200 nM OXA after treatment with 10 µM or 20 µM CBD, respectively.
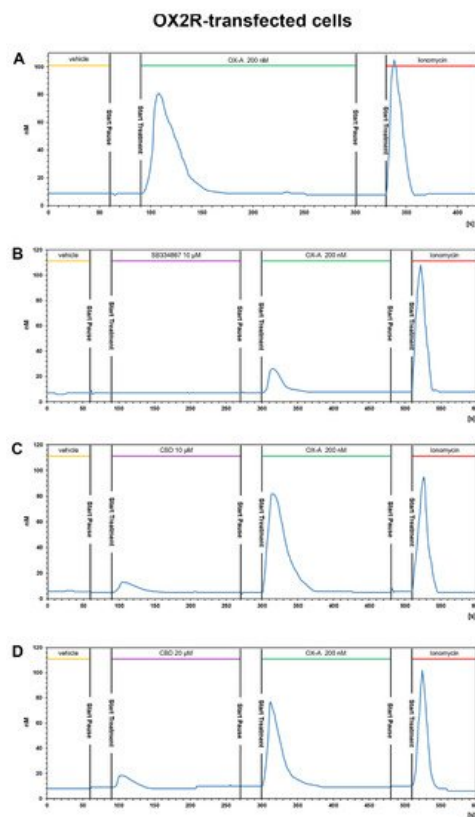
Figure 5. CBD does not alter the OX-A-induced $[Ca^{2+}]_i$ increase in CHO cells stably transfected with OX2R. Representative traces of single-cell $[Ca^{2+}]_i$ response in Fura-2- loaded CHO cells stably overexpressing OX2R and treated with 200 nM OXA, alone or in combination with 10µM SB334867 or with 10 µM or 20 µM CBD Ionomycin (2 µM) was added at the end of the experiment. Images, collected continuously for 420 s (**A**,**B**) or 600 s (**C**,**D**), were analyzed by

the Leica MetaMorph software for calcium imaging to quantify the intracellular $[Ca^{2+}]_i$ increase expressed as 340/387nm excitation ratio between calcium-bound Fura-2 (green cells) and calcium-free Fura-2 (red cells). (**A**) 200 nM OX-A increases $[Ca^{2+}]_i$ in cells. (**B**) The OX1R antagonist SB334867 prevents the OX-A-induced $[Ca^{2+}]_i$ enhancement in the cells. (**C,D**) Treatment with 20 µM or 10 µM CBD, respectively, has no effect on the increase of $[Ca^{2+}]_i$ induced by OX-A.

2.3.2. CBD Inhibits the Ca²⁺ Response Induced by OX-A in OX1R, but Not in OX2R Transfected CHO Cells

The presence of CBD 10 µM or 20 µM for ~3 min in the calcium-containing extracellular solution (see methods section) of CHO cells stably expressing OX1R caused a slight enhancement of $[Ca^{2+}]_i$ and was able to reduce (10 µM) or prevent (20 µM) the $[Ca^{2+}]_i$ increase induced by 200 nM OX-A (**Figure 4**C,D). As shown in **Figure 4**C, 10 µM CBD induced a slight $[Ca^{2+}]_i$ peak ($[Ca^{2+}]_i$: 18.1 ± 2.7 nM vs. basal $[Ca^{2+}]_i$: 6 ± 1.2 nM; $p < 0.05$) and reduced the increment of $[Ca^{2+}]$ induced by subsequent treatment with OX-A ($[Ca^{2+}]_i$: 30.5 ± 3.6 nM vs. basal $[Ca^{2+}]_i$: 6 ± 1.2 nM; $p < 0.05$). Pretreatment with 20 µM CBD increased the $[Ca^{2+}]$ (peak $[Ca^{2+}]_i$: 23.7 ± 2.9 nM vs. basal $[Ca^{2+}]_i$: 8.9 ± 1.3nM; $p < 0.05$), but the $[Ca^{2+}]_i$ recorded in cells with 200 nM OX-A after CBD treatment was similar to the basal levels (10.8 ± 2.2 nM for OX-A vs. 8.9 ± 1.3 nM for the vehicle-treated cells; $p > 0.05$) (**Figure 4**D). These results suggest that CBD acts as OX1R antagonist.

On the contrary, pretreatment with 10 µM or 20 µM CBD of CHO cells stably expressing OX2R did not inhibit the Ca²⁺ response induced by 200 nM OX-A. As shown in **Figure 5**C,D, CBD induced elevation of $[Ca^{2+}]_i$ in a concentration-dependent manner (12.2 ± 1.3 nM for CBD 10 µM vs. basal level: 5.8 ± 1.6 nM; 17.9 ± 2.3 nM for CBD 20 µM vs. basal level: 7.9 ± 1.9 nM; $p < 0.05$), whereas the addition of OX-A in the same cell medium after 180 s of CBD treatment induced a $[Ca^{2+}]_i$ enhancement with a peak of $[Ca^{2+}]_i$ significantly higher than the basal $[Ca^{2+}]_i$ ($[Ca^{2+}]_i$: 82.3 ± 5.9 nM after CBD 10µM vs. basal level: 5.8 ± 1.6 nM; 77.5 ± 6.3 nM after CBD 20 µM vs. basal level: 7.9 ± 1.9 nM; $p < 0.001$). The elevation of $[Ca^{2+}]_i$ induced by CBD, as already observed in calcium mobilization assay, is not due to OXRs, since it also occurs in non-transfected cells (see **Figure 6**).
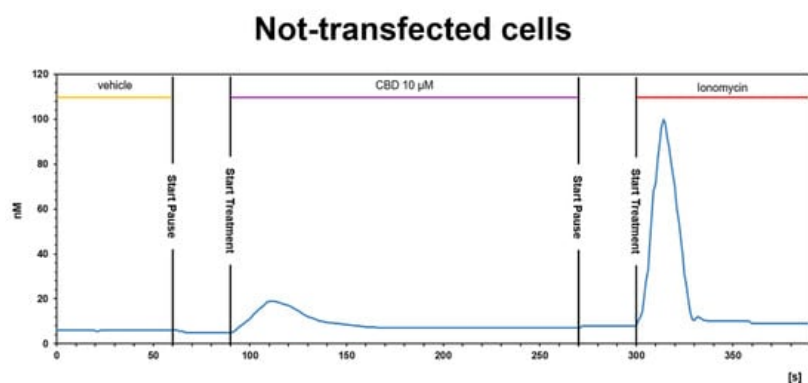

Figure 6. CBD induces a slight $[Ca^{2+}]_i$ increase in not-transfected CHO cells. Representative traces of single-cell $[Ca^{2+}]_i$ response in Fura-2- loaded not-transfected CHO cells. Ionomycin (2 µM) was added at the end of the experiment. Images, collected continuously for 390 s, were analyzed by the Leica MetaMorph software for calcium imaging to quantify the intracellular $[Ca^{2+}]_i$ increase expressed as 340/387 nm excitation ratio between calcium-bound Fura-2 (green cells) and calcium-free Fura-2 (red cells).

Collectively, the functional assays carried out by both intracellular Ca²⁺ measurements and Ca²⁺ imaging showed that CBD is an OX1R antagonist at low micromolar concentrations and is selective for OX1R over OX2R.

### 3.4. OX1R/CBD Theoretical Complex

Next, a comparative study of molecular docking and molecular dynamics simulations (MD) in membrane environment (up to 200 ns) of CBD in complex with either OX1R or OX2R was undertaken to shed light on the binding mode of CBD in the binding site of OX1R and to rationalize CBD selectivity toward this receptor over OX2R. From docking runs of CBD into the OX1R binding site, four starting poses were selected for the subsequent MD on the basis of binding energy and ability to interact with residues known to be relevant for receptor binding and, among these, three final poses, termed I, II, and III, were stable to MD in terms of root-mean-square-deviation (rmsd). The first two poses shared a similar arrangement, only differing for a slight rotation of the CBD aromatic ring. However, since only pose I formed a stable H-bond with Ser103[2.61], pose II was discarded from subsequent analysis. In pose I, the terpenoid ring interacted with Pro123[3.29], a residue involved in ligand interactions also in experimentally determined complex structures, while the pentanoyl chain pointed toward Phe219[5.42]. In pose III CBD adopted a reverse orientation with respect to pose I, with the pentanoyl chain pointing toward the receptor N-terminal end and the terpenoid ring pointing toward Ala127[3.33], Tyr215[5.38], and Phe219[5.42]. Pose I and III, representative of the possible binding modes of CBD within the orthosteric binding site of OX1R, are shown

in **Figure 7**, panel a and b, respectively. It is noteworthy that OX1R residues interacting with CBD have been previously characterized as being important for antagonist binding to this receptor [25].
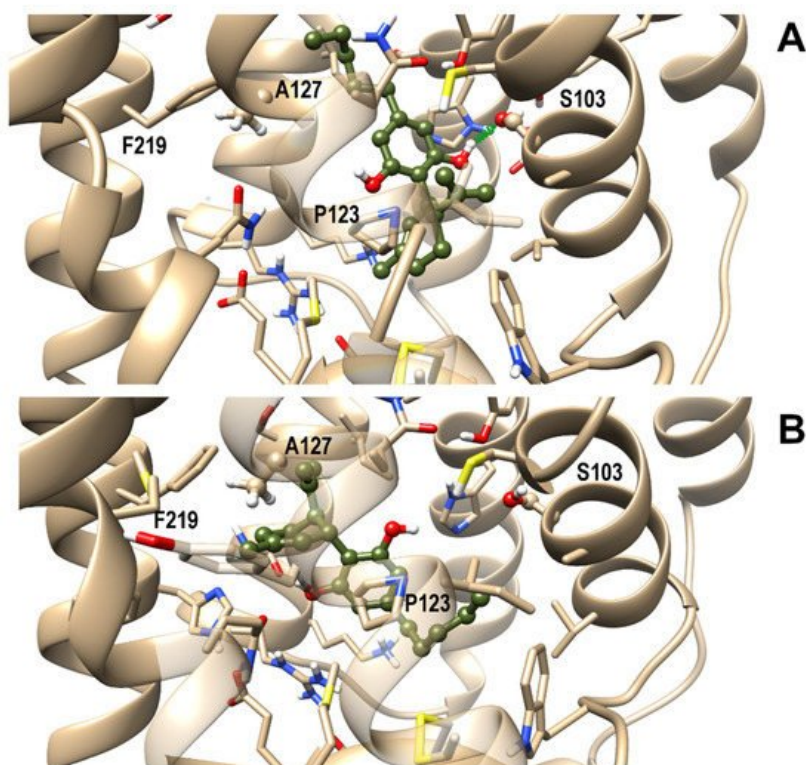

Figure 7. Representative frames from MD of CBD/OX1R complexes: Pose I (**A**) and III (**B**). A ball and stick representation is used for heavy atoms plus polar hydrogens of ligand, whereas a stick representation was used for protein sidechains within 5 Å from the ligand. Protein carbon atoms are colored in tan according to ribbon for protein and olive drab for the ligand. Hydrogen, nitrogen, oxygen, and sulfur atoms are painted white, blue, red and yellow, respectively. A transparent surface for ribbons is used whenever they hide the ligand. A "green spring" style is adopted for H-bonds involving ligand atoms.

A best-fit superposition of protein backbones between CBD poses I/III and the x-ray structure of the OX1R in complex with the antagonist suvorexant (**Figure 8**, panels A and B, respectively) shows that, when overlapping the two ligand poses, CBD globally spans the same spatial region occupied by suvorexant, each pose filling about one-half of the volume of the bulkier suvorexant. Hence, the reduced occupancy of the binding site and the higher flexibility of CBD in comparison to suvorexant account for CBD's lower potency vs. suvorexant (K_i 0.55 nM) [32].
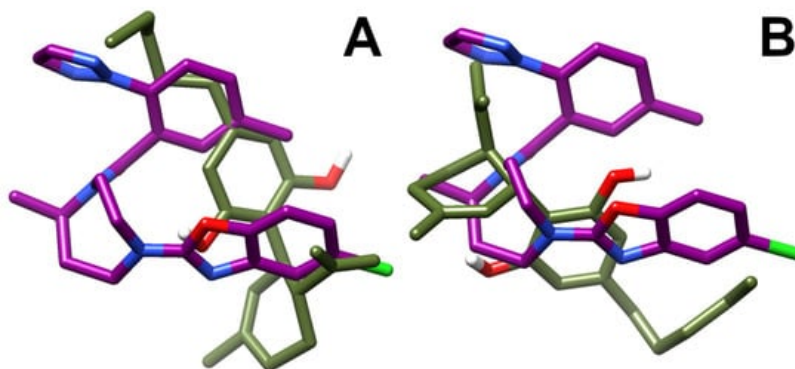
Figure 8. Best-fit superposition of protein backbones between CBD poses I (**A**)/III (**B**) and the x-ray structure of the OX1R-suvorexant complex. Only the ligands are shown for clarity and drawn in stick representation. The suvorexant is colored in deep purple and the CBD in olive drab. Hydrogen, nitrogen, oxygen, and fluorine atoms are painted white, blue, red and green, respectively.

To assess if the arrangements found for CBD could also be conserved in OX2R, the same starting poses I and III were used for MD of CBD/OX2R complexes. The first pose was also found as the best docking pose in OX2R whereas pose III was not found, due to steric clashes with $Thr135^{3.33}$. Trajectory analysis, reported in **Figure 9**, showed that neither pose I, nor pose III resulted in stable OX2R, thus explaining the receptor selectivity of CBD toward OX1R.
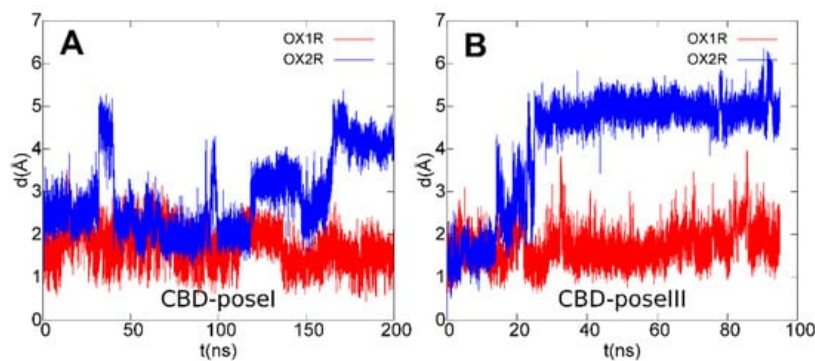
Figure 9. Root mean square deviation (rmsd) plots of CBD ligand in poses I (**A**)/III (**B**) during the last 200 ns (**A**)/95 ns (**B**) of MD simulations after best-fit of protein backbone in OX1R (red) and OX2R (blue).

In fact, among the contacting residues in the OX1R binding site, CBD formed stable interactions with the only two non-conserved residues between OX1R and OX2R, that is OX1R Ser103$^{2.61}$ (pose I) and OX1R Ala127$^{3.33}$ (pose III), both replaced by a bulkier threonine residue in OX2R, which contributed to the destabilization of the CBD–OX2R complex during MD simulations, in agreement with the results from the binding assays. Furthermore, the docking/MD study identified a protein–ligand interaction network involving OX1R residues reported to be critical for antagonist binding, in agreement with the experimental validation.

3. Conclusions

In summary, we identified CBD as a selective OX1R antagonist and such effect could contribute to explaining, for example, the anorexigenic effect exerted by CBD reported in some studies [33], since OX1R is localized in appetite-regulating neurons in the hypothalamus [34] and it has been demonstrated that the hyperphagia induced by the centrally administrated OX-A is mediated by OX1Rs [35][36]. Moreover, the selective OX1R antagonist SB-334867 attenuates orexin-A induced feeding and has anorectic effects inducing satiety without nausea [37].

Although further studies are required to assess the clinical relevance of orexin antagonism CBD action, this study adds a new element to the complex picture of the mechanism of action of CBD and paves the way to in vivo studies fully exploring the pharmacological implications of its activity as a negative modulator of the hypocretinergic–endocannabinoid axis, for example in the treatment of substance use disorders or body weight regulation.

References

1. Mandolini, G.M.; Lazzaretti, M.; Pigoni, A.; Oldani, L.; Delvecchio, G.; Brambilla, P. Pharmacological properties of cannabidiol in the treatment of psychiatric disorders: A critical overview. Epidemiol. Psychiatr. Sci. 2018, 27, 327–335.

2. Ożarowski, M.; Karpiński, T.M.; Zielińska, A.; Souto, E.B.; Wielgus, K. Cannabidiol in neurological and neoplastic diseases: Latest developments on the molecular mechanism of action. Int. J. Mol. Sci. 2021, 22, 4294.

3. Ibeas Bih, C.; Chen, T.; Nunn, A.V.W.; Bazelot, M.; Dallas, M.; Whalley, B.J. Molecular targets of cannabidiol in neurological disorders. Neurotherapeutics 2015, 12, 699–730.

4. Vitale, R.M.; Iannotti, F.A.; Amodeo, P. The (Poly)pharmacology of cannabidiol in neurological and neuropsychiatric disorders: Molecular mechanisms and targets. Int. J. Mol. Sci. 2021, 22, 4876.

5. De Petrocellis, L.; Ligresti, A.; Moriello, A.S.; Allarà, M.; Bisogno, T.; Petrosino, S.; Stott, C.G.; Di Marzo, V. Effects of cannabinoids and cannabinoid-enriched Cannabis extracts on TRP channels and endocannabinoid metabolic enzymes. Br. J. Pharmacol. 2011, 163, 1479–1494.

6. Ryberg, E.; Larsson, N.; Sjögren, S.; Hjorth, S.; Hermansson, N.-O.; Leonova, J.; Elebring, T.; Nilsson, K.; Drmota, T.; Greasley, P.J. The orphan receptor GPR55 is a novel cannabinoid receptor. Br. J. Pharmacol. 2009, 152, 1092–1101.

7. Campos, A.C.; Ferreira, F.R.; Guimarães, F.S. Cannabidiol blocks long-lasting behavioral consequences of predator threat stress: Possible involvement of 5HT1A receptors. J. Psychiatr. Res. 2012, 46, 1501–1510.

8. Kathmann, M.; Flau, K.; Redmer, A.; Tränkle, C.; Schlicker, E. Cannabidiol is an allosteric modulator at mu- and delta-opioid receptors. Naunyn. Schmiedebergs. Arch. Pharmacol. 2006, 372, 354–361.

9. Laprairie, R.B.; Bagher, A.M.; Kelly, M.E.M.; Denovan-Wright, E.M. Cannabidiol is a negative allosteric modulator of the cannabinoid CB 1 receptor. Br. J. Pharmacol. 2015, 172, 4790–4805.

10. Tham, M.; Yilmaz, O.; Alaverdashvili, M.; Kelly, M.E.M.; Denovan-Wright, E.M.; Laprairie, R.B. Allosteric and orthosteric pharmacology of cannabidiol and cannabidiol-dimethylheptyl at the type 1 and type 2 cannabinoid receptors. Br. J. Pharmacol. 2019, 176, 1455–1469.

11. Straiker, A.; Dvorakova, M.; Zimmowitch, A.; Mackie, K. Cannabidiol inhibits endocannabinoid signaling in autaptic hippocampal neurons. Mol. Pharmacol. 2018, 94, 743–748.

12. Gonzalez-Cuevas, G.; Martin-Fardon, R.; Kerr, T.M.; Stouffer, D.G.; Parsons, L.H.; Hammell, D.C.; Banks, S.L.; Stinchcomb, A.L.; Weiss, F. Unique treatment potential of cannabidiol for the prevention of relapse to drug use: Preclinical proof of principle. Neuropsychopharmacology 2018, 43, 2036–2045.

13. Prud'homme, M.; Cata, R.; Jutras-Aswad, D. Cannabidiol as an intervention for addictive behaviors: A systematic review of the evidence. Subst. Abus. Res. Treat. 2015, 9, 33–38.

14. Hurd, Y.L.; Yoon, M.; Manini, A.F.; Hernandez, S.; Olmedo, R.; Ostman, M.; Jutras-Aswad, D. Early phase in the development of cannabidiol as a treatment for addiction: Opioid relapse takes initial center stage. Neurotherapeutics 2015, 12, 807–815.

15. Perrey, D.A.; Zhang, Y. Therapeutics development for addiction: Orexin-1 receptor antagonists. Brain Res. 2018, 9, 587–602.

16. Jantti, M.H.; Putula, J.; Turunen, P.M.; Nasman, J.; Reijonen, S.; Lindqvist, C.; Kukkonen, J.P. Autocrine endocannabinoid signaling through CB1 receptors potentiates OX1 orexin receptor signaling. Mol. Pharmacol. 2013, 83, 621–632.

17. Jäntti, M.; Putula, J.; Somerharju, P.; Frohman, M.; Kukkonen, J. OX 1 orexin/hypocretin receptor activation of phospholipase D. Br. J. Pharmacol. 2012, 165, 1109–1123.

18. Li, J.; Hu, Z.; de Lecea, L. The hypocretins/orexins: Integrators of multiple physiological functions. Br. J. Pharmacol. 2014, 171, 332–350.

19. Saito, Y.C.; Maejima, T.; Nishitani, M.; Hasegawa, E.; Yanagawa, Y.; Mieda, M.; Sakurai, T. Monoamines inhibit GABAergic neurons in ventrolateral preoptic area that make direct synaptic connections to hypothalamic arousal neurons. J. Neurosci. 2018, 38, 6366–6378.

20. Hasegawa, E.; Yanagisawa, M.; Sakurai, T.; Mieda, M. Orexin neurons suppress narcolepsy via 2 distinct efferent pathways. J. Clin. Investig. 2014, 124, 604–616.

21. Cristino, L.; Busetto, G.; Imperatore, R.; Ferrandino, I.; Palomba, L.; Silvestri, C.; Petrosino, S.; Orlando, P.; Bentivoglio, M.; Mackie, K.; et al. Obesity-driven synaptic remodeling affects endocannabinoid control of orexinergic neurons. Proc. Natl. Acad. Sci. USA 2013, 110, 2229–2238.

22. Peyron, C.; Tighe, D.K.; van den Pol, A.N.; de Lecea, L.; Heller, H.C.; Sutcliffe, J.G.; Kilduff, T.S. Neurons containing hypocretin (orexin) project to multiple neuronal systems. J. Neurosci. 1998, 18, 9996–10015.

23. Scammell, T.E.; Winrow, C.J. Orexin receptors: Pharmacology and therapeutic opportunities. Annu. Rev. Pharmacol. Toxicol. 2011, 51, 243–266.

24. Merlo Pich, E.; Melotto, S. Orexin 1 receptor antagonists in compulsive behavior and anxiety: Possible therapeutic use. Front. Neurosci. 2014, 8, 26.

25. Yin, J.; Babaoglu, K.; Brautigam, C.A.; Clark, L.; Shao, Z.; Scheuermann, T.H.; Harrell, C.M.; Gotter, A.L.; Roecker, A.J.; Winrow, C.J.; et al. Structure and ligand-binding mechanism of the human OX1 and OX2 orexin receptors. Nat. Struct. Mol. Biol. 2016, 23, 293–299.

26. Yin, J.; Mobarec, J.C.; Kolb, P.; Rosenbaum, D.M. Crystal structure of the human OX2 orexin receptor bound to the insomnia drug suvorexant. Nature 2015, 519, 247–250.

27. Flores, Á.; Maldonado, R.; Berrendero, F. Cannabinoid-hypocretin cross-talk in the central nervous system: What we know so far. Front. Neurosci. 2013, 7, 256.

28. Imperatore, R.; Palomba, L.; Morello, G.; Spiezio, A.D.; Piscitelli, F.; Marzo, V.D.; Cristino, L. Formation of OX-1R/CB1R heteromeric complexes in embryonic mouse hypothalamic cells: Effect on intracellular calcium, 2-arachidonoyl-glycerol biosynthesis and ERK phosphorylation. Pharmacol. Res. 2016, 111, 600–609.

29. Taylor, L.; Gidal, B.; Blakey, G.; Tayo, B.; Morrison, G. A phase I, randomized, double-blind, placebo-controlled, single ascending dose, multiple dose, and food effect trial of the safety, tolerability and pharmacokinetics of highly purified cannabidiol in healthy subjects. CNS Drugs 2018, 32, 1053–1067.

30. Eubler, K.; Herrmann, C.; Tiefenbacher, A.; Köhn, F.-M.; Schwarzer, J.; Kunz, L.; Mayerhofer, A. Ca2+ signaling and IL-8 secretion in human testicular peritubular cells involve the cation channel TRPV2. Int. J. Mol. Sci. 2018, 19, 2829.

31. Olivas-Aguirre, M.; Torres-López, L.; Valle-Reyes, J.S.; Hernández-Cruz, A.; Pottosin, I.; Dobrovinskaya, O. Cannabidiol directly targets mitochondria and disturbs calcium homeostasis in acute lymphoblastic leukemia. Cell Death Dis. 2019,

10, 779.

32. Cox, C.D.; Breslin, M.J.; Whitman, D.B.; Schreier, J.D.; McGaughey, G.B.; Bogusky, M.J.; Roecker, A.J.; Mercer, S.P.; Bednar, R.A.; Lemaire, W.; et al. Discovery of the dual orexin receptor antagonist [(7 R)-4-(5-Chloro-1,3-benzoxazol-2-yl)-7-methyl-1,4-diazepan-1-yl][5-methyl-2-(2H -1,2,3-triazol-2-yl)phenyl] methanone (MK-4305) for the treatment of insomnia. J. Med. Chem. 2010, 53, 5320–5332.

33. Ignatowska-Jankowska, B.; Jankowski, M.M.; Swiergiel, A.H. Cannabidiol decreases body weight gain in rats: Involvement of CB2 receptors. Neurosci. Lett. 2011, 490, 82–84.

34. Bäckberg, M.; Hervieu, G.; Wilson, S.; Meister, B. Orexin receptor-1 (OX-R1) immunoreactivity in chemically identified neurons of the hypothalamus: Focus on orexin targets involved in control of food and water intake. Eur. J. Neurosci. 2002, 15, 315–328.

35. Rodgers, R.J.; Halford, J.C.G.; de Nunes Souza, R.L.; de Canto Souza, A.L.; Piper, D.C.; Arch, J.R.S.; Upton, N.; Porter, R.A.; Johns, A.; Blundell, J.E. SB-334867, a selective orexin-1 receptor antagonist, enhances behavioural satiety and blocks the hyperphagic effect of orexin-A in rats. Eur. J. Neurosci. 2001, 13, 1444–1452.

36. Haynes, A.C.; Jackson, B.; Overend, P.; Buckingham, R.E.; Wilson, S.; Tadayyon, M.; Arch, J.R. Effects of single and chronic intracerebroventricular administration of the orexins on feeding in the rat. Peptides 1999, 20, 1099–1105.

37. Ishii, Y.; Blundell, J.; Halford, J.; Upton, N.; Porter, R.; Johns, A.; Jeffrey, P.; Summerfield, S.; Rodgers, R. Anorexia and weight loss in male rats 24h following single dose treatment with orexin-1 receptor antagonist SB-334867. Behav. Brain Res. 2005, 157, 331–341.